Micro-Raman spectroscopy of a single freestanding GaN nanorod grown by molecular beam epitaxy

Ching-Lien Hsiao,[a] Li-Wei Tu,[b] Tung-Wei Chi,[c] and Min Chen
Department of Physics, National Sun Yat-Sen University, Kaohsiung, Taiwan 80424, Republic of China and Center for Nanoscience and Nanotechnology, National Sun Yat-Sen University, Kaohsiung, Taiwan 80424, Republic of China

Tai-Fa Young
Department of Mechanical and Electro-Mechanical Engineering, National Sun Yat-Sen University, Kaohsiung, Taiwan 80424, Republic of China and Center for Nanoscience and Nanotechnology, National Sun Yat-Sen University, Kaohsiung, Taiwan 80424, Republic of China

Chih-Ta Chia
Department of Physics, National Taiwan Normal University, Taipei 116, Taiwan, Republic of China

Yu-Ming Chang
Center for Condensed Matter Sciences, National Taiwan University, Taipei 106, Taiwan, Republic of China

(Received 17 October 2006; accepted 18 December 2006; published online 22 January 2007)

Micro-Raman spectra were measured on a single freestanding GaN nanorod, which was grown by molecular beam epitaxy. A sharp linewidth of E_2(high) mode of 2.1 cm^{-1} measured in the $x(y,y)\bar{x}$ configuration indicates the high crystalline quality of the nanorod. The angle-dependent Raman spectroscopy shows that the integrated intensities of these first-order Raman modes follow the theoretical sinusoidal functions. The forbidden E_1(LO) mode that appeared in the $x(z,z)\bar{x}$ scattering configurations is assigned to the quasi-LO phonon mode. Power-dependent Raman spectroscopy shows redshift with increasing laser power density due to sample heating which is confirmed by Stokes and anti-Stokes measurements. The broadband centered at 708.5 cm^{-1} is ascribed to the surface mode of the nanostructure. © *2007 American Institute of Physics*.
[DOI: 10.1063/1.2433034]

Although GaN-based light emitters have been successfully commercialized, large amount of dislocations is still a big threat to the lifetime and the yield of the devices.[1] To reduce the dislocation density for higher quality, many methods have been proposed. We have reported the growth of dislocation-free GaN nanorod in previous work.[2] These quasi-one-dimensional, high-quality nanorods could be potential templates for high-performance nanodevices such as light-emitting diodes, laser diodes, photodetectors, etc.[3–6] Previous studies on the optical properties of one-dimensional GaN nanostructures were mostly measured on a bundle of nanorods or entangled nanowires,[7–9] and only few reports focused on individual nanowires.[10] In this work, we report the results of polarized micro-Raman spectroscopy study of a single freestanding, high-quality GaN nanorod with no other peaks except ~3.4 eV transition in photoluminescence measurement, which was grown by plasma-assisted molecular beam epitaxy on Si(111) substrates.[2,11] These GaN nanorods are all vertically aligned to the substrate, with the c axis along the growth direction, and show well-faceted hexagonal shape. To elucidate the phonon behaviors in nanorods, the dependence of the Raman shift on the angle between the laser polarization direction and the rod c axis is investigated. The results agree well with the theoretical calculation of the first-order Raman modes. We have also investigated the dependence of the Raman shift on the excitation laser power density. The Stokes and the anti-Stokes measurements yield an estimate of the temperature increase of the nanorod due to the heat generated by the laser irradiation. Surface phonon mode, because of the large surface area and the excellent surface quality of the nanorod, is presented.

Micro-Raman spectroscopy (Jobin-Yvon T64000, 0.35 cm^{-1} resolution) was performed on a single freestanding GaN nanorod on quartz template via backscattering geometry at room temperature. A linear polarized neodymium-doped yttrium aluminum garnet 532 nm laser was used to be the excitation source. The laser was focused through a microscope into a spot of about 1 μm in diameter. The polarization direction of incident light was controlled using a half-wave plate, and the polarization of scattered light was selected through the triple gratings equipped in the spectrometer, which only pass light polarized in the horizontal direction. In this work, the reference frame (x,y,z) is fixed on the rod with the z axis pointing along the crystallographic c axis of the rod, and the direction of laser polarization is rotated against the rod. As plotted in the inset of Fig. 1(a), θ (φ) is the angle between the laser polarization and the z axis (x axis). The representations of $\theta=0°$ and $\theta=90°$ scattering configurations with $\varphi=90°$ are $x(z,z)\bar{x}$ and $x(y,y)\bar{x}$, respectively, in the Porto notation.[12] Figure 1(a) is the result of the angle-dependent Raman spectroscopy. All the A_1(TO), E_1(TO), and E_2(high) modes appear prominently at $\theta=45°$, and with a dominant A_1(TO) line at 0° and E_2(high) at 90°.[12,13] At lower power densities, they are located at 531.1, 557.8, and 567.2 cm^{-1}, respectively. The frequencies of these

[a]Present address: Center for Condensed Matter Sciences, National Taiwan University, Taipei 106, Taiwan.
[b]Electronic mail: lwtu@mail.nsysu.edu.tw
[c]Present address: Industrial Technology Research Institute, Hsin-Chu 310, Taiwan.

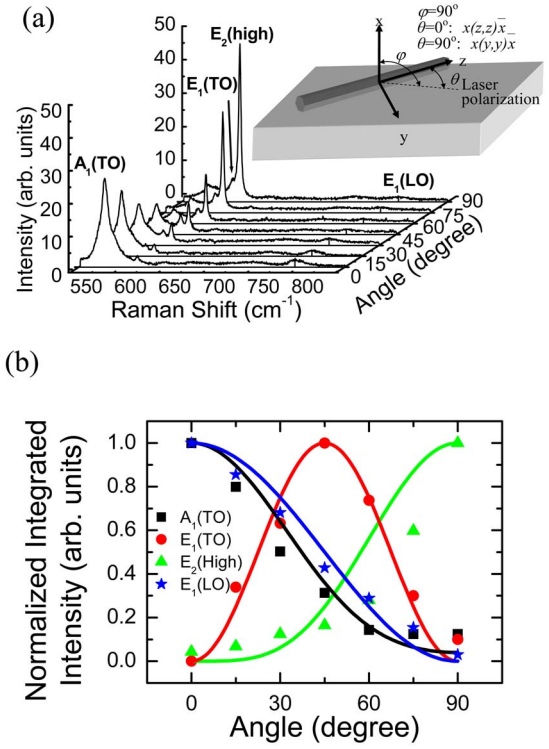

FIG. 1. (Color online) (a) Angle-dependent Raman spectroscopy is measured at different angles between the laser polarization and the rod length (c axis). The inset shows a schematic diagram of the Raman scattering configurations measured on a single freestanding nanorod. (b) Normalized integrated intensity in all phonon modes. Scattered symbols are experimental data and solid lines are theoretical fitting.

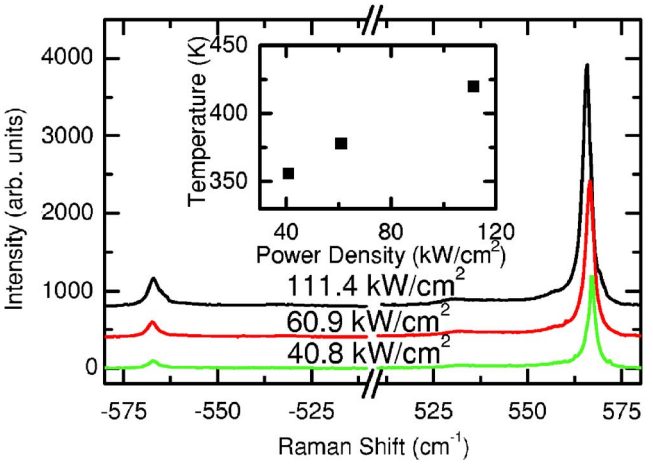

FIG. 2. (Color online) Stokes and anti-Stokes lines were measured to estimate the nanorod temperature with various laser power densities. The estimated temperatures of the nanorod from I_{AS}/I_S calculations are plotted in the inset.

phonon modes are consistent with those obtained by Raman spectroscopy measurements of the bulk and the thin film GaN in the same scattering configuration. A sharp linewidth of E_2(high) mode of 2.1 cm^{-1} manifests the high crystalline quality of the nanorod, which is consistent with our previous study on transmission electron microscopy.[2] The selection-rule forbidden E_1(LO) mode, located at 742.5 cm^{-1}, is barely seen at lower angles. This E_1(LO)-like mode has been assigned as a quasi-LO mode or the resonance Raman mode induced by the Fröhlich interaction in the literature.[13–15] In this work, because the excitation laser energy of 2.33 eV (532 nm) is far below the GaN band gap of 3.42 eV, the resonance Raman effect is very hard to be induced under this excitation so that it is more likely the quasi-LO mode.[13,14]

Normalized integrated intensities of all the modes are plotted in the Fig. 1(b). From the Raman intensity I as $I \sim |\hat{e}_S \cdot R \cdot \hat{e}_L|^2$, where R is the Raman tensor of the scattering process[12] and $\hat{e}_L(\hat{e}_S)$ the unit vector of the incident (scattered) light polarization, which can be expressed by the unit vectors of x, y, and z axes as $\hat{e}_L(\hat{e}_S)=\cos\varphi\hat{x}+\sin\theta\sin\varphi\hat{y}+\cos\theta\sin\varphi\hat{z}$, the Raman intensities can be expressed as $I(A_1) \propto (a\sin^2\theta+\cos^2\theta)^2$, $I(E_1(y)) \propto \sin^2 2\theta$, $I(E_1(x)) \propto \cos^2\theta$ and $I(E_2) \propto \sin^4\theta$, as the angle $\varphi \to \pi/2$. According to the theoretical calculation and consideration of phonon propagation, the Raman intensities of the A_1(TO), E_1(TO), and E_2(high) modes, i.e., $I(A_1)$, $I(E_1(y))$, and $I(E_2)$, respectively, in the Fig. 1(b) match well the theoretical calculation curves. Although the trend of E_1(LO)-like mode shows a similar trend to the A_1(TO) mode rather than the E_1(TO) mode, it does not follow the A_1(TO) mode. The intensity of E_1(LO)-like mode should follow the $I(E_1(x))$ with the functional dependence of $\cos^2\theta$, which is forbidden when the phonon propagation is strictly parallel or perpendicular to the c axis.[12–14] The above results suggest that the single nanorod offers an opportunity for applications on angle-selective nanosensors.

In order to gain more insight into the phonon behaviors in a single nanorod, the laser-power-density dependent Raman spectra were taken at $\theta=45°$ which was chosen to obtain all the modes. A largest redshift of $\sim$1.6 cm^{-1} for all modes is obtained when the power density is increased to 111.4 kW/cm^2. These shifts are mainly due to the lattice expansion caused by the heating effect through the laser irradiation. In the mean time, the linewidth shows similar behavior and becomes broader with increasing laser power density. The integrated intensities of Raman peaks show a linear dependence on the laser power density, which is due to the increase of the stimulated phonon population with the increasing laser power density. Among them, the intensity of A_1(TO) mode has the largest rate of increase in the intensity (largest slope of the linear relation) which is 4.1, 4.8, and 7.6 times larger than the E_1(TO), E_2(high), and E_1(LO) modes, respectively. This indicates that the rate of change of polarizability along the polar axis is higher than the nonpolar crystal plane.

The Stokes and the anti-Stokes Raman spectroscopy was employed to estimate the rod temperature during laser irradiation. In Fig. 2, the laser power densities vary from 40.6 to 111.4 kW/cm^2 at $\theta=90°$ to optimize the E_2(high) signals. According to the quantum theory with a classical frequency factor,[16] the relative integrated intensity between the anti-Stokes and the Stokes Raman shift is given by $I_{\text{anti-Stokes}}/I_{\text{Stokes}}=((\omega+\omega_v)/(\omega-\omega_v))^4 e^{-\hbar\omega_v/kT}$, where ω is the laser frequency, ω_v the lattice vibrational frequency, $\hbar=h/2\pi$ with the Plank constant h, k the Boltzmann constant, and T the absolute temperature. The rod temperatures estimated from the E_2(high) mode are about 356, 378, and 420 K at 40.8, 60.9, and 111.4 kW/cm^2, respectively. The nanorod temperatures estimated from the ratios of I_{AS}/I_S of the E_2(high) mode are plotted in the inset of Fig. 2. The shifts of the E_2(high) are due to the phonon-phonon and the phonon-electron interactions.[17] At higher laser power density, the excess heat is produced due to the creation of large

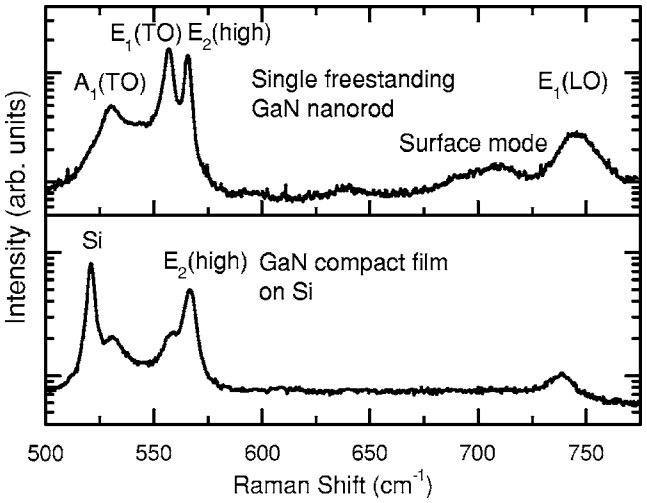

FIG. 3. Micro-Raman spectra were measured from a single freestanding GaN nanorod and a compact GaN thin film. A prominent peak at 708.5 cm^{-1} is contributed from the surface vibrational mode of GaN nanorod. All samples were measured in the $x(x+y,x+y)\bar{x}$ scattering configuration to obtain all main Raman peaks.

amount of phonons and the poor thermal conductivity of the nanocrystal.[18]

In Fig. 3, Raman spectra were measured on a single freestanding GaN nanorod and a GaN thin film on Si substrate. A semilogarithmic diagram is plotted. A new prominent phonon mode appeared at the lower frequency side of E_1(LO) mode for the single nanorod which is absent for the compact thin film. This new mode is well separated from the E_1(LO) mode and centered at 708.5 cm^{-1}. With a largest surface-to-volume ratio and well-defined hexagonal cylindrical shape with highly crystalline structure,[2] it is assigned as the surface mode of GaN nanocrystals rather than the disorder-active Raman scattering which referred to the defects effect of crystal or *a*-GaN. This surface-related mode in polar materials (the Fröhlich mode) was reported in a porous GaN film before.[19,20] The surface mode frequency ω_s can be described as $\omega_s^2=\{[\varepsilon_o+\varepsilon_m(1/S-1)]/[\varepsilon_\infty+\varepsilon_m(1/S-1)]\}\omega_{\mathrm{TO}}^2$,[21] where ω_{TO} is the frequency of the optical phonon, $\varepsilon_o(\varepsilon_\infty)$ the static (high-frequency) dielectric constant, ε_m the dielectric constant of the surrounding medium which is 1 for air, and *S* the depolarization factor which depends on the particle shape. From the Lyddane-Sache-Teller relation, $\omega_{\mathrm{LO}}^2/\omega_{\mathrm{TO}}^2=\varepsilon_o/\varepsilon_\infty$, the LO-TO splitting of E_1 mode gives a static dielectric constant of $\varepsilon_o=9.4$ using $\varepsilon_\infty=5.3$.[13] A suitable *S* number of 3/7 is chosen for ellipsoid,[21] and this yields a surface phonon frequency $\omega_s=708.7\ cm^{-1}$ which is very close to the measured value.

Micro-Raman spectroscopy on a single freestanding GaN nanorod grown by MBE has been demonstrated. The self-assembled GaN nanorod is of single crystalline wurtzite phase with a hexagonal geometrical shape. A_1(TO), E_1(TO), and E_2(high) vibrational modes are well resolved in the $x(x+y,x+y)\bar{x}$ scattering configuration. The results of the angle-dependent Raman spectroscopy suggest that the single nanorod offers an opportunity for applications on angle-selective nanosensors. Power-dependent Raman spectroscopy shows redshift and line broadening of the Raman lines with increasing laser power density, which is ascribed to the temperature increase estimated from Stokes and anti-Stokes line measurements. Integrated line intensity depends linearly on the power density with the A_1(TO) mode having a much higher rate of change than the other modes. A new peak at 708.5 cm^{-1} is ascribed to the surface mode due to the high surface-to-volume ratio and the high perfection of the hexagonal surfaces of the nanostructure, which agrees well with the calculated value.

This work was supported by the National Science Council of the Republic of China.

[1] H. Morkoç, *Nitride Semiconductor and Devices* (Springer, New York, 2000), Chap. 5, p. 150.
[2] L. W. Tu, C. L. Hsiao, T. W. Chi, I. Lo, and K. Y. Hsieh, Appl. Phys. Lett. **82**, 1601 (2003).
[3] S. Chattopadhyay, S. C. Shi, Z. H. Lan, C. F. Chen, K. H. Chen, and L. C. Chen, J. Am. Chem. Soc. **127**, 2820 (2005).
[4] C. L. Hsiao, L. W. Tu, M. Chen, Z. W. Jiang, N. W. Fan, Y. J. Tu, and K. R. Wang, Jpn. J. Appl. Phys., Part 2 **44**, L1076 (2005).
[5] F. Qian, Y. Li, S. Gradečak, D. Wang, C. J. Barrelet, and C. M. Liber, Nano Lett. **4**, 1975 (2004).
[6] J. Ristic, E. Calleja, A. Trampert, S. Fernández-Garrido, C. Rivera, U. Jahn, and K. H. Ploog, Phys. Rev. Lett. **94**, 146102 (2005).
[7] H. L. Liu, C. C. Chen, C. T. Chia, C. C. Yeh, C. H. Chen, M. Y. Yu, S. Keller, and S. P. DenBarrs, Chem. Phys. Lett. **345**, 245 (2001).
[8] H. W. Seo, S. Y. Bae, J. Park, H. Yang, K. S. Park, and S. Kim, J. Chem. Phys. **115**, 9492 (2002).
[9] H. W. Seo, Q. Y. Chen, M. N. Iliev, L. W. Tu, C. L. Hsiao, J. K. Mean, and W. K. Chu, Appl. Phys. Lett. **88**, 153124 (2006).
[10] P. J. Pauzauskie, D. Talaga, K. Seo, P. T. Yang, and F. Lagugné-Labarthet, J. Am. Chem. Soc. **127**, 17146 (2005).
[11] C. L. Hsiao, L. W. Tu, T. W. Chi, H. W. Seo, Q. Y. Chen, and W. K. Chu, J. Vac. Sci. Technol. B **24**, 845 (2006).
[12] C. A. Arguello, D. L. Rousseau, and S. P. S. Porto, Phys. Rev. **181**, 1351 (1969).
[13] T. Azuhata, T. Sota, K. Suzuki, and S. Nakarmura, J. Phys.: Condens. Matter **7**, L129 (1995).
[14] L. Bergman, M. Dutta, C. Balkas, R. F. Davis, J. A. Christman, D. Alexson, and R. J. Nemanich, J. Appl. Phys. **85**, 3535 (1999).
[15] D. Behr, J. Wagner, J. Schneider, H. Amano, and I. Akasaki, Appl. Phys. Lett. **68**, 2404 (1996).
[16] N. B. Colthup, L. H. Daly, and S. E. Wiberley, *Introduction to Infrared and Raman Spectroscopy* (Academic, New York, 1990), Chap. 1, p. 65.
[17] M. S. Liu, L. A. Bursill, S. Prawer, K. W. Nugent, Y. Z. Tong, and G. Y. Zhang, Appl. Phys. Lett. **74**, 3125 (1999).
[18] S. Piscanec, M. Cantoro, A. C. Ferrari, J. A. Zapien, Y. Lifshitz, S. T. Lee, S. Hofmann, and J. Robertson, Phys. Rev. B **68**, 241312(R) (2003).
[19] I. M. Tiginyanu, A. Sarua, G. Irmer, J. Monecke, S. M. Hubbard, D. Pavlidis, and V. Valiaev, Phys. Rev. B **64**, 233317 (2001).
[20] A. Sarua, J. Monecke, G. Irmer, I. M. Tiginyanu, G. Gärtner, and H. L. Hartnagel, J. Phys.: Condens. Matter **13**, 6687 (2001).
[21] S. Hayashi and H. Kanamori, Phys. Rev. B **26**, 7079 (1997).